**Zeitschrift:** Eclogae Geologicae Helvetiae

Herausgeber: Schweizerische Geologische Gesellschaft

**Band:** 87 (1994)

**Heft:** 2: Pollution and pollutant transport in the geosphere, a major

environmental issue: symposium held during the 173rd annual meeting

of the Swiss Academy of Natural Sciences

**Artikel:** Repeated change from crustal shortening to orogen-parallel extension

in the Austroalpine units of Graubünden

**Autor:** Froitzheim, Nikolaus / Schmid, Stefan M. / Conti, Paolo

**Kapitel:** 3: Alpine deformation of the southwestern Silvretta, Ela and Err-

Carungas nappes

**DOI:** https://doi.org/10.5169/seals-167471

#### Nutzungsbedingungen

Die ETH-Bibliothek ist die Anbieterin der digitalisierten Zeitschriften auf E-Periodica. Sie besitzt keine Urheberrechte an den Zeitschriften und ist nicht verantwortlich für deren Inhalte. Die Rechte liegen in der Regel bei den Herausgebern beziehungsweise den externen Rechteinhabern. Das Veröffentlichen von Bildern in Print- und Online-Publikationen sowie auf Social Media-Kanälen oder Webseiten ist nur mit vorheriger Genehmigung der Rechteinhaber erlaubt. Mehr erfahren

#### **Conditions d'utilisation**

L'ETH Library est le fournisseur des revues numérisées. Elle ne détient aucun droit d'auteur sur les revues et n'est pas responsable de leur contenu. En règle générale, les droits sont détenus par les éditeurs ou les détenteurs de droits externes. La reproduction d'images dans des publications imprimées ou en ligne ainsi que sur des canaux de médias sociaux ou des sites web n'est autorisée qu'avec l'accord préalable des détenteurs des droits. En savoir plus

### Terms of use

The ETH Library is the provider of the digitised journals. It does not own any copyrights to the journals and is not responsible for their content. The rights usually lie with the publishers or the external rights holders. Publishing images in print and online publications, as well as on social media channels or websites, is only permitted with the prior consent of the rights holders. Find out more

**Download PDF:** 02.12.2025

ETH-Bibliothek Zürich, E-Periodica, https://www.e-periodica.ch

Jurassic, and by the widespread occurrence of basement clasts in Middle to Upper Jurassic breccias. (4) The Platta nappe, including ophiolites and thin slivers of continental basement, Triassic and Jurassic sedimentary rocks in Austroalpine facies, representing an oceanic domain between the margin s. str. and the Margna-Sella continental fragment. (5) The Margna-Sella system, continental basement with a Mesozoic sedimentary cover in Austroalpine facies, derived from a continental fragment that became separated from the margin by extensional faulting in the Middle Jurassic. This fragment may have been connected to the Austroalpine farther south. (6) The Malenco-Forno-Lizun ophiolites of the South Penninic ocean.

All these units together form the "orogenic lid" (Laubscher 1983), a nappe pile that was assembled in the Cretaceous and that overrode the deeper Penninic units as a coherent thrust mass during the Early Tertiary. The lid includes not only Austroalpine units but also the South Penninic ophiolite units mentioned above (Liniger & Nievergelt 1990).

Bernina and Err systems are traditionally termed Lower Austroalpine. The Margna-Sella system may be referred to as "Ultrapenninic" following a suggestion by Trümpy (1992). Following Liniger (1992), we assume that the present position of the Platta ophiolites between the Lower Austroalpine above and the Margna-Sella system below does not result from Alpine backfolding or backthrusting but reflects the original paleogeographic arrangement of these units. The Ela nappe is Upper Austroalpine according to most authors (e. g. Spicher 1972) but belongs to the Lower Austroalpine Bernina system in our view (Schmid & Froitzheim 1993, see also chapter 5.2).

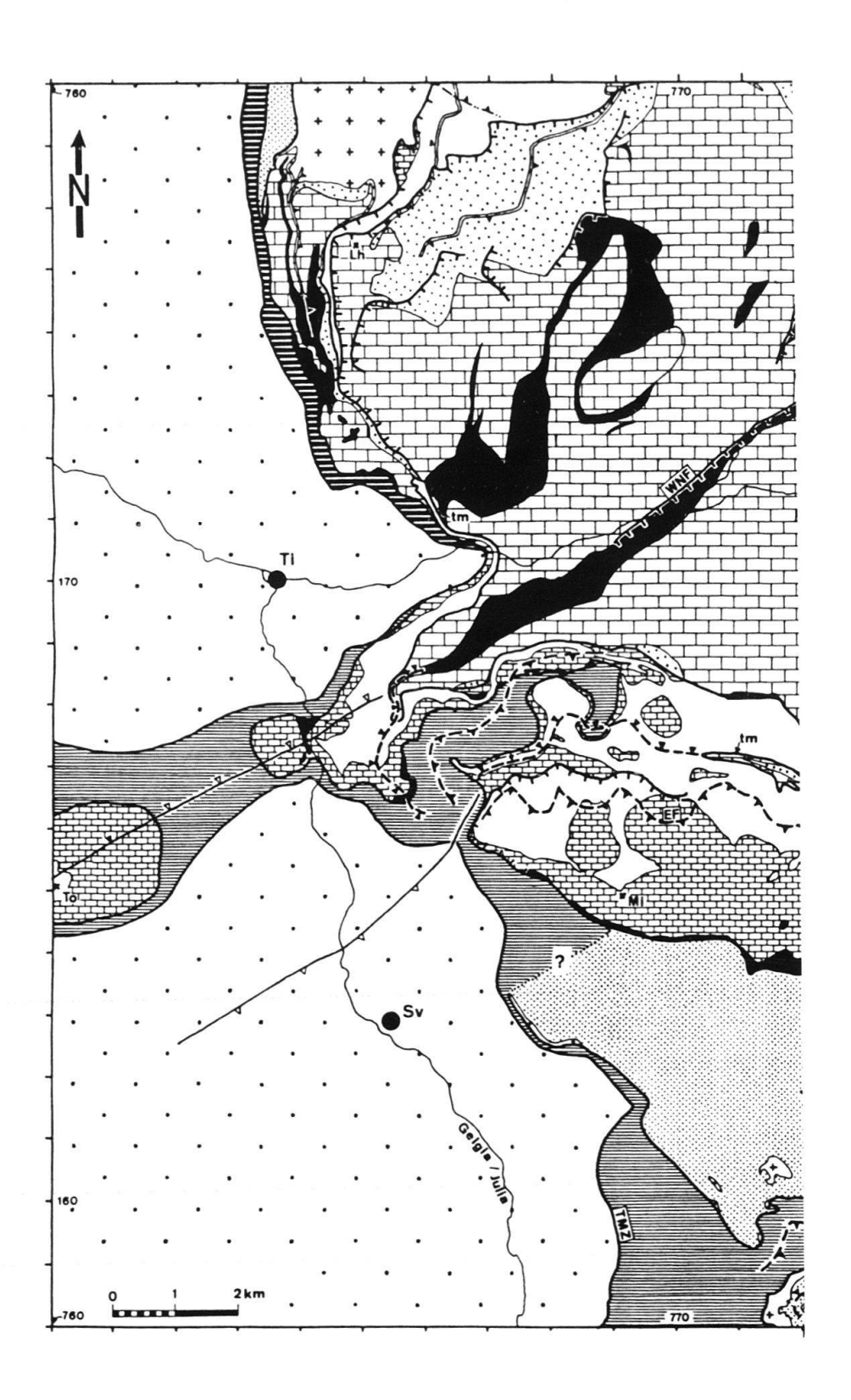
### 3 Alpine deformation of the southwestern Silvretta, Ela and Err-Carungas nappes

In the following, an area of the Austroalpine nappe edifice west of the Engadine line is described in detail (Fig. 2). The structural architecture of this area records the sequence of Alpine deformation events in a particularly clear way.

In this area, three major tectonic units of the Austroalpine are exposed (Figs. 1, 2): Silvretta nappe, Ela nappe and Err-Carungas nappe. The Silvretta nappe is a large Upper Austroalpine thrust sheet consisting predominantly of basement rocks, mostly gneiss and amphibolite. Cover rocks of Permian to Late Triassic age are only preserved at its southwestern edge in the Landwasser and Ducan synclinal areas (Fig. 1). Along its southern border, the Silvretta nappe is underlain by the Ela nappe, a detached and folded thrust sheet of Upper Triassic dolomite and Lower Jurassic to Cretaceous shale and limestone, lacking rocks older than Late Triassic. The Ela nappe is underlain by the Err-Carungas

Fig. 1. (a) Tectonic map of the Austroalpine and underlying upper Penninic nappes in Graubünden. Small triangles along tectonic boundaries point in the direction of the structurally higher unit, without indicating the nature of the boundary (some are not thrusts but low-angle normal faults). A Dol, Arosa dolomites; Cv, Corvatsch nappe; Me, Mezzaun unit; Mu, Murtiröl unit; Pg, Phyllitgneiss zone; Rh, Rothorn nappe; Sz, Samedan zone; Ts, Tschirpen nappe; GL, Gallo line; ST, Schlinig thrust; TBT, Trupchun-Braulio thrust; TMZ, Turba mylonite zone; ZT, Zebru thrust; (Ch), Chur; (Da), Davos; (St), St. Moritz; (Tr), Val Trupchun.

<sup>(</sup>b) Reconstructed east-west cross-section of the southeastern continental margin of the South Penninic ocean in the Late Jurassic and boundaries of the main Alpine tectonic units. Geometry of continent-ocean transition reconstructed assuming tectonic denudation of subcontinental mantle along top-west extensional detachment faults, according to model of Lemoine et al. (1987). For further explanation see text.



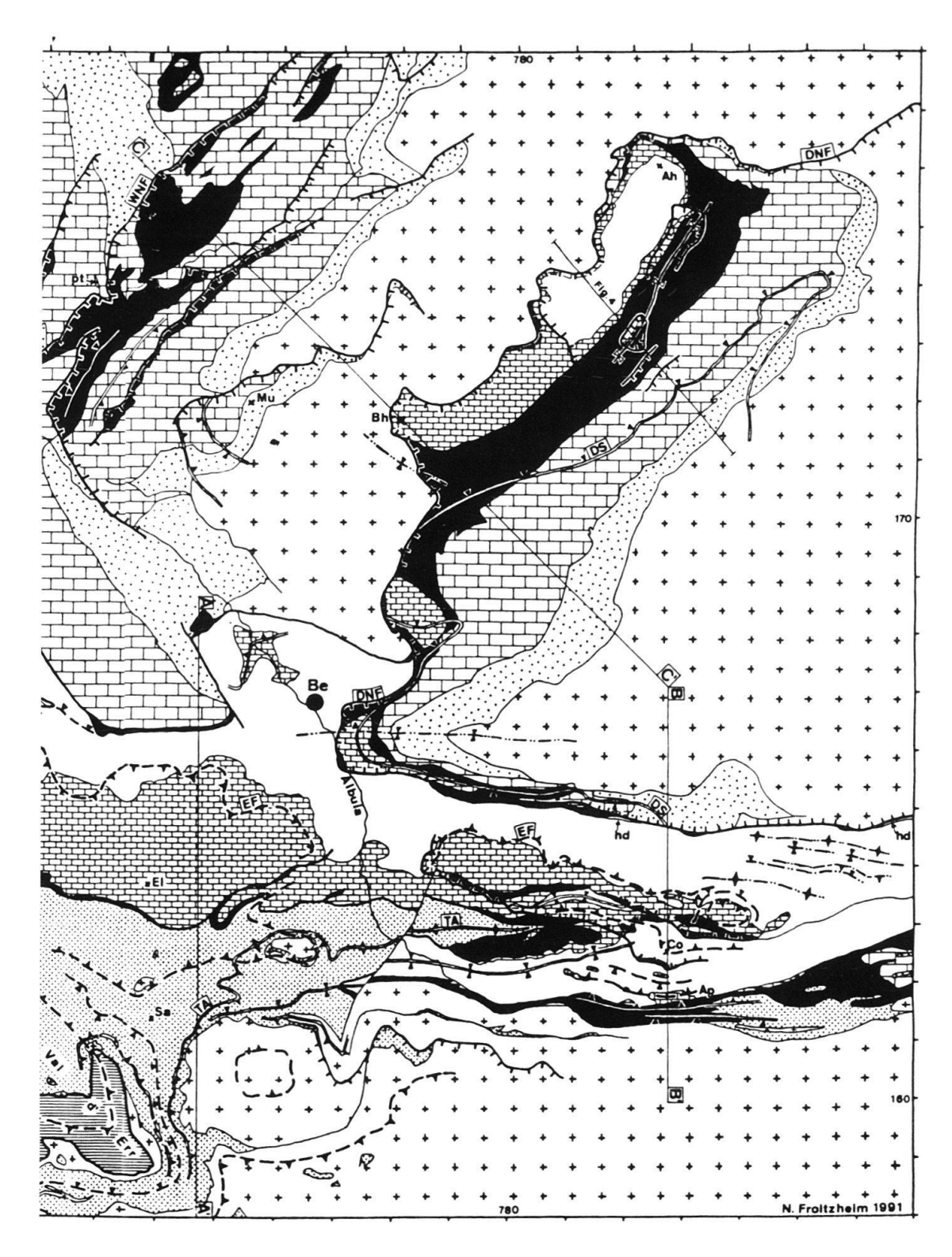
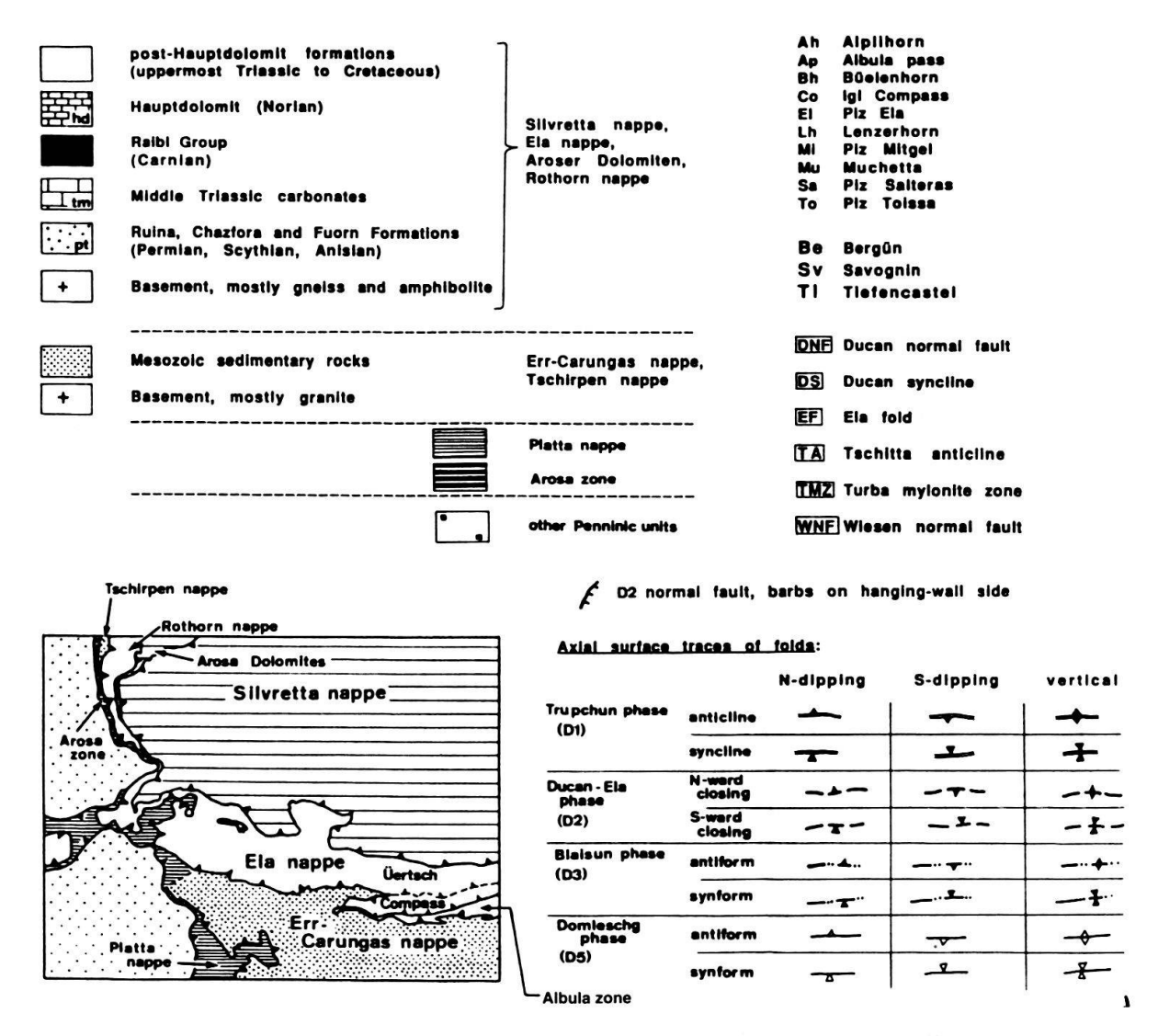


Fig. 2. Tectonic map of the southwestern Silvretta nappe, Ela nappe and northern Err-Carungas nappe. Geological base map compiled using maps of Brauchli & Glaser (1922), Frei & Ott (1926), Eugster & Frei (1927), Eugster & Leupold (1930), Cornelius (1932), Bearth et al. (1935), Stöcklin (1949), unpublished maps by D. Bollinger, M. Eberle, G. P. Eberli, U. Eichenberger, S. Frank, H. Furrer, T. Gronowski, H. Lozza, A. Rohrbach, M. Weh, D. Wurster and own mapping.



Legend for Fig. 2 (p. 566/567).

nappe, belonging to the Err system of the Lower Austroalpine nappes. This nappe includes pre-Mesozoic basement as well as a cover series of Permian to Cretaceous age. East of the Albula pass (southeastern corner of map. Fig. 2), an additional, minor unit its

East of the Albula pass, (southeastern corner of map, Fig. 2), an additional, minor unit its exposed between the Ela nappe above and the Err-Carungas nappe below, the Albula zone (Eggenberger 1926, Heierli 1955). This is a stack of thin, imbricated slivers comprising stratigraphic series from pre-Permian basement to Carnian evaporite, and occasionally also Jurassic and possibly Cretaceous strata (see Fig. 5a in Schmid & Froitzheim 1993). From the Albula pass towards the west, the Albula zone is only represented by a thin layer of Carnian cargneule at the base of the Ela nappe. Still further to the west, this layer becomes indiscernible from the basal cargneule of the Ela nappe.

Tectonic contacts between the three major thrust sheets (from top to bottom: Silvretta, Ela, Err-Carungas) are steeply north-dipping or subvertical (e. g. Fig. 3b). Hence this

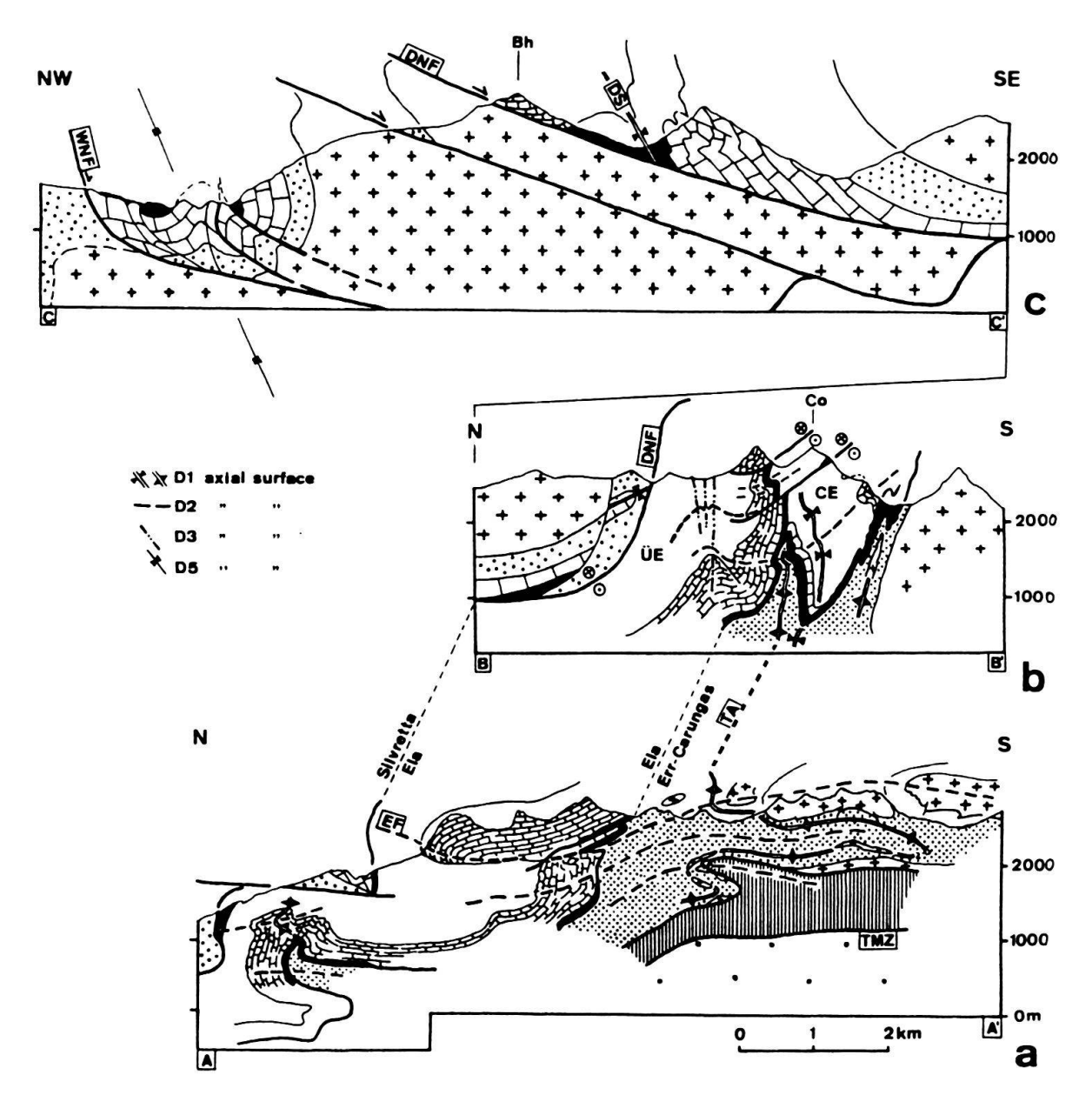


Fig. 3. Profiles from the Silvretta through the Ela into the northern Err-Carungas nappe. Profile traces and legend in Fig. 2. CE, Compass element, ÜE, Üertsch element of the Ela nappe.

stack of imbricates is now found side by side, with the highest unit to the north. Upper Penninic units appear under the Austroalpine in the western part of the map (Fig. 2): the Platta nappe to the south and the Arosa zone to the north. Both units comprise ophiolites derived from oceanic crust of the South Penninic ocean.

In the following, the structures observed in the three thrust sheets are described, proceeding from top (Silvretta nappe) to base (Err-Carungas nappe). A short general description precedes the structural analysis of each nappe.

## 3.1 Southwestern Silvretta nappe (Ducan area)

## 3.1.1 General description

The Ducan area of the Silvretta nappe (NE part of map, Fig. 2) is characterized by a Permian to Upper Triassic sedimentary cover series, preserved in a northeast-trending syncline (Duncan syncline). The syncline is bordered on both sides by pre-Mesozoic basement. The sedimentary sequence of the Ducan area comprises volcanoclastic and clastic Permian to Lower Triassic rocks, Middle Triassic dolomite and limestone, evaporite-bearing Raibl Group of Carnian age, Hauptdolomit (Norian), and Kössen Formation (Rhaetian), preserved in the core of the syncline (Eugster 1923, Eichenberger 1986). The syncline faces northwest. Its northwestern, normal limb is strongly attenuated or cut off by normal faults. The Mesozoic formations of this northwestern limb overlie the basement along a tectonic contact, the Ducan normal fault (Figs. 3c, 4). In contrast, the southeastern, vertical to overturned limb is well preserved, only cut by minor normal faults. The transgressive contact of Permian on basement is still preserved in this limb.

At the southwestern termination of the Ducan syncline, the Permo-Mesozoic fill of the syncline directly rests on the Ela nappe, and the Silvretta basement is omitted. West

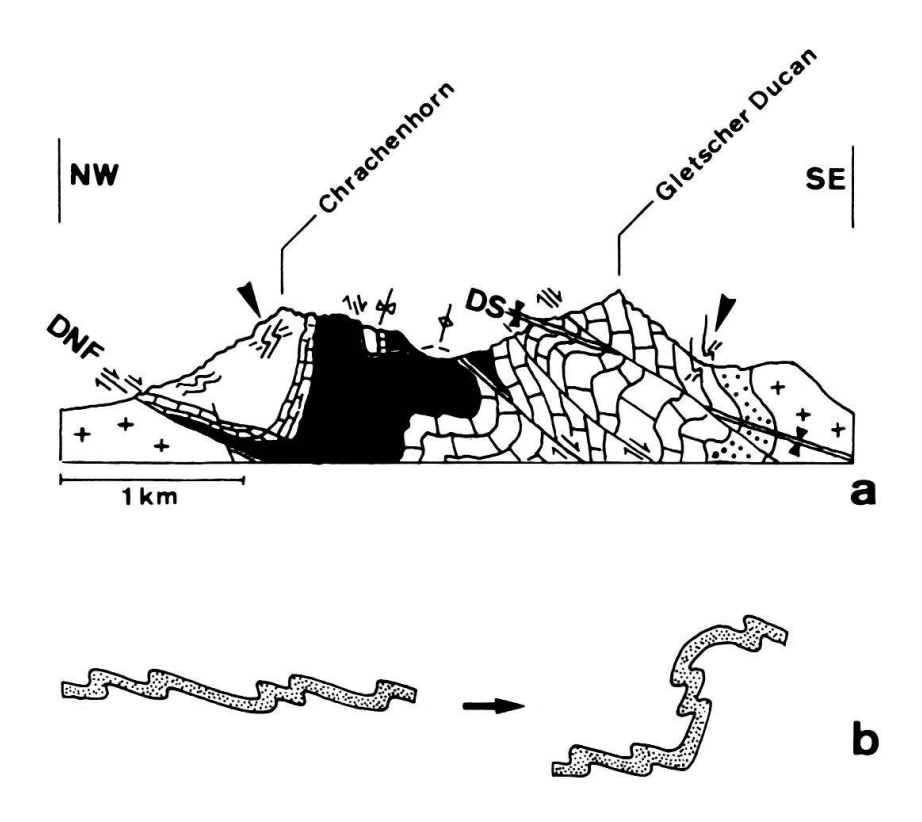


Fig. 4. (a) Cross-section of the central part of the Ducan syncline, after Eichenberger (1986), Wurster (1991) and own observations (trace of section in Fig. 2, same legend same as Fig. 2). DS, axial trace of D<sub>1</sub> Ducan syncline, DNF, Ducan normal fault. Solid arrows indicate minor folds with "wrong" vergence relative to large-scale folds. Southeast-dipping normal faults, including the Ducan normal fault, crosscut the D<sub>1</sub> folds. The syncline-anticline pair in the middle of the section, deforming the normal fault, is tentatively correlated with late NE-striking folds (Domleschg phase).

(b) Explanation for vergence of  $D_1$  folds: Minor folds were slightly earlier formed and subsequently rotated during formation of large scale folds. This is interpreted as two stages in a continuous process.

and East of the Ducan syncline, however, the Silvretta basement reappears. This peculiar situation was interpreted by Trümpy (1980, p. 80) in the following way: the Silvretta nappe was first folded (Ducan syncline, Landwasser syncline) and then detached and transported westward along a thrust which truncated the base of the two synclines. As we will show below, we arrive at a slightly different picture: the southwestern Silvretta nappe shows the imprints of early thrusting and folding followed by normal faulting. Finally, the normal faults were deformed in a second folding event.

# 3.1.2 D<sub>1</sub> folding and thrusting in the Silvretta nappe

Minor folds with amplitudes of 10 to 100 metres are observed in the Ducan syncline (Fig. 4 and profiles in Eugster 1923, Eichenberger 1986, Furrer et al. 1992). The folds have northeast- to north-trending axes and generally face northwest to west. They are associated with an axial plane cleavage in limestones and shales of the Middle and Upper Triassic, representing the oldest penetrative deformational structure in the sedimentary rocks of the Ducan area. Most of the minor folds can be interpreted as parasitic folds of the Ducan syncline. However, in at least two localities the folds have the wrong vergence in respect to their position in the syncline (folds indicated by thick arrows in Fig. 4a). The enveloping surfaces of the folds in these localities are vertical to overturned, that is, southeast-dipping. The axial surfaces of the folds dip northwest, and the facing direction is downward and northwest. In the absence of superposition criteria, these folds can be interpreted as originally northwest-vergent folds that were subsequently rotated anticlockwise, looking northeast, when the large-scale Ducan syncline developed into its final shape (Fig. 4b). This is supported by the observation that "wrong-vergence" folds are restricted to steep to overturned limbs of the major folds. Although this interpretation implies a slightly older age for these minor folds in respect to the Ducan syncline, it is assumed that both were generated during the same process of west- to northwest directed shearing deformation  $(D_1)$ .

Towards the southwestern termination of the Ducan syncline, the strike of minor D<sub>1</sub> folds changes from northeast to north and eventually northwest (Spitz & Dyhrenfurth 1913). The same is true for the hinge of the Ducan syncline which thus describes a westward-convex arc, one of the "Rhaetic arcs" of Spitz & Dyhrenfurth (1913). Therefore, sedimentary rocks of the Ducan syncline can be followed towards the east and along the base of the Silvretta nappe into the area north of Albula pass (Fig. 2). The bending of the fold axes is not smooth but associated with intense brittle deformation (Eugster 1923, p. 101).

A northwest- to west-trending stretching lineation was found in strongly sheared Permian to Lower Triassic sandstones and conglomerates of the Ducan syncline in Val Tisch (coord. 782.8/164.7) and in the Landwasser area, northwest of the Ducan syncline (coord. 767.35/177.05). This lineation is interpreted to approximate the shearing direction during  $D_1$  folding. Hence,  $D_1$  folding is related to the west- to northwestward directed transport of the Silvretta nappe.

### 3.1.3 D<sub>2</sub> normal faulting in the Silvretta nappe

The Ducan area, like the southwestern Silvretta nappe in general, is cut by numerous southwest- to south-striking, southeast- to east-dipping faults. Offset of marker horizons

generally indicates southeast-directed normal fault movement (Figs. 3c, 4). The most important of these faults is the Ducan normal fault or "Ducan-Scherfläche" of Eugster (1923), forming the northwestern boundary of the sedimentary rocks of the Ducan syncline. The Ducan normal fault cuts obliquely through the Ducan syncline, as can be seen in map view (Fig. 2) from the truncation of the axial trace of the syncline (DS) by the Ducan normal fault (DNF) northeast of Bergün. This relation indicates that the normal fault overprints and therefore postdates the Ducan syncline. This is confirmed by small-scale overprinting relations, like normal-fault-related drag folds deforming the D<sub>1</sub> cleavage (Wurster 1991).

Geometric relations along the southern continuation of the Ducan normal fault indicate that normal faulting not only postdates D<sub>1</sub> folding but also the emplacement of the Silvretta nappe on top of the Ela nappe. At a triple point 2 km northeast of Bergün, the Ducan normal fault truncates the basal thrust of the Silvretta nappe (small insert map in Fig. 5, see also Fig. 2). The contour lines of both faults in Figure 5 show that the normal fault ("A") does not change its orientation at this triple point and that the Silvretta basal thrust ("B") ends abruptly against the normal fault. South of the triple point, the Ducan normal fault changes its orientation from a southeastward dip into a steep northward dip, thus outlining an eastward-plunging synform (D<sub>3</sub> fold, see below). Further towards east, the Ducan normal fault continues in a north-dipping orientation along the base of the Silvretta nappe. This tectonic boundary ("C") is interpreted as representing the Silvretta basal thrust, reactivated by the Ducan normal fault. According to this interpretation, the Ducan normal fault formed as an east-dipping, listric fault with a steeper upper segment that cut through the Silvretta nappe, and a lower, shallowly dipping segment that followed the basal thrust of the nappe. The part of the Silvretta nappe located in the hanging wall of the Ducan normal fault slipped back towards east. Thereby the sediments of the Ducan syncline were downthrown directly onto the Ela nappe and the Silvretta basement was omitted.

# 3.1.4 Fault rocks from the Ducan normal fault and the base of the Silvretta nappe

In order to test the hypothesis outlined above, namely that the Ducan fault represents a top-east to -southeast directed normal fault which partly reactivated the basal thrust of the Silvretta nappe, we investigated microstructures in fault rocks along the Ducan normal fault at Büelenhorn and along the Silvretta-Ela boundary north and northeast of Albula pass.

On the west side of Büelenhorn (Fig. 3c), the hanging wall of the Ducan normal fault consists of Upper Triassic Hauptdolomit and the footwall of pre-Permian orthogneiss ("younger orthogneiss", Maggetti & Flisch 1993). Along the contact between dolomite above and gneiss below, a thin layer of strongly sheared fault rocks is exposed. The lower part of this, 40 cm thick, is cataclasite derived from Permian to Lower Triassic clastic rocks. The upper part, 1 to 2 meters thick, is intensely sheared limestone (Middle Triassic S-charl Formation). The preservation of a normal, although extremely thinned stratigraphic sequence suggests that deformation was ductile on the scale of the fault zone.

The fault rock shown in Figure 6a, derived from limestone of the S-charl formation, has an irregular, anastomosing foliation oriented roughly parallel to the shear zone boundaries. It exhibits a weak, east-southeast trending slickenside lineation. The plane of the

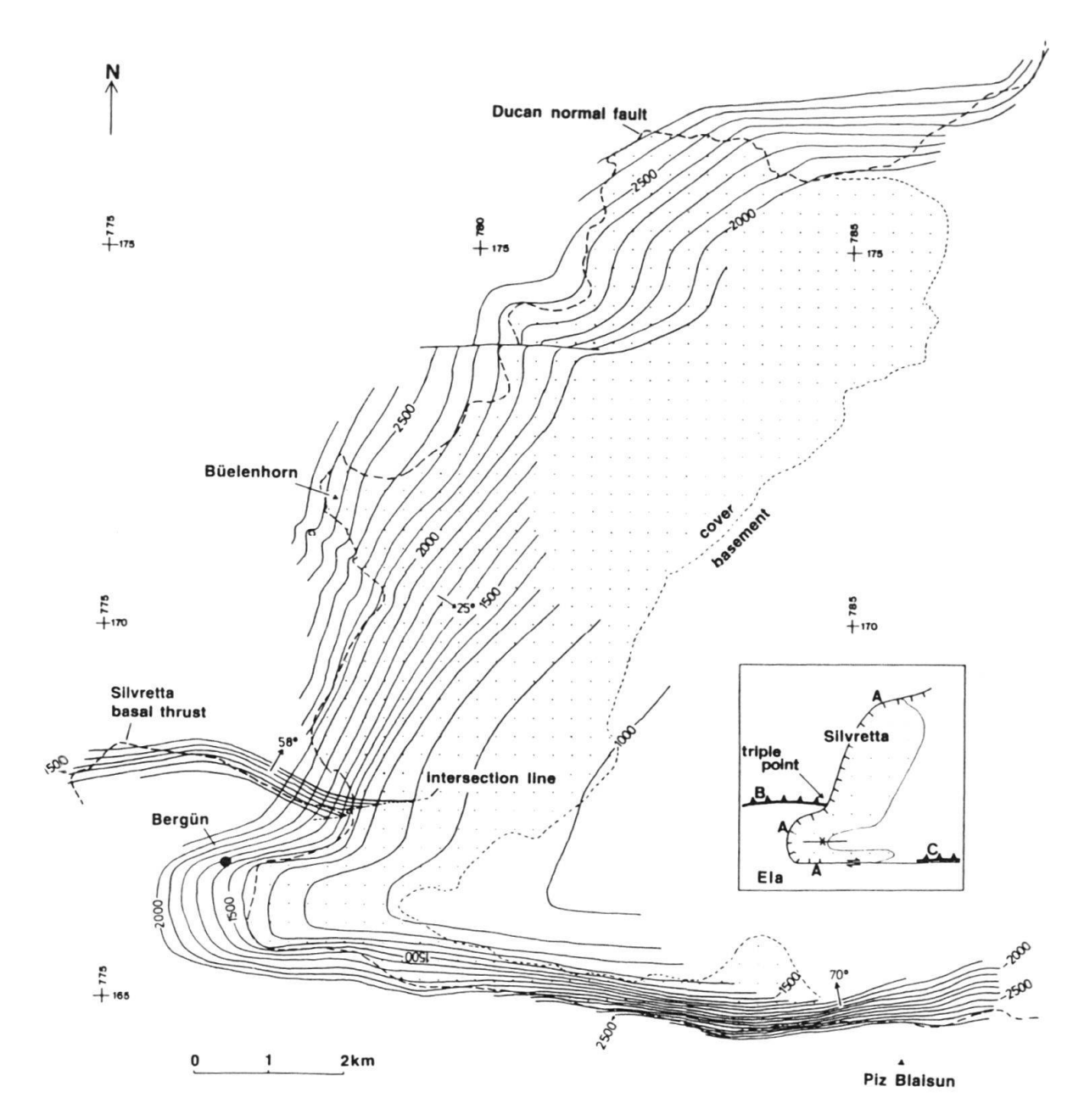


Fig. 5. Contour map of the Ducan normal fault (small insert map: A) and the basal thrust of the Silvretta nappe (B). (C) is the basal thrust, reactivated by the Ducan normal fault. Note truncation of the Silvretta basal thrust by the Ducan normal fault at triple point, and folding of the Ducan normal fault around an east-striking  $D_3$  fold. Numbers along contour lines indicate elevation in metres above sea level, arrows with numbers indicate dip direction and angle of tectonic boundaries.

section is perpendicular to the foliation and parallel to the slickenside lineation. Stylolites and calcite veins are abundant in this rock. Two types of veins can be distinguished: first, extension veins filled with calcite crystals showing no signs of deformation  $(v_1)$ , and second, calcite veins strongly overprinted by cataclastic shearing  $(v_2)$ . The unsheared veins of the first type are generally at high angles to the fault-zone boundaries, whereas most of the sheared veins are at lower angles to the fault-zone boundaries. The stylolites are

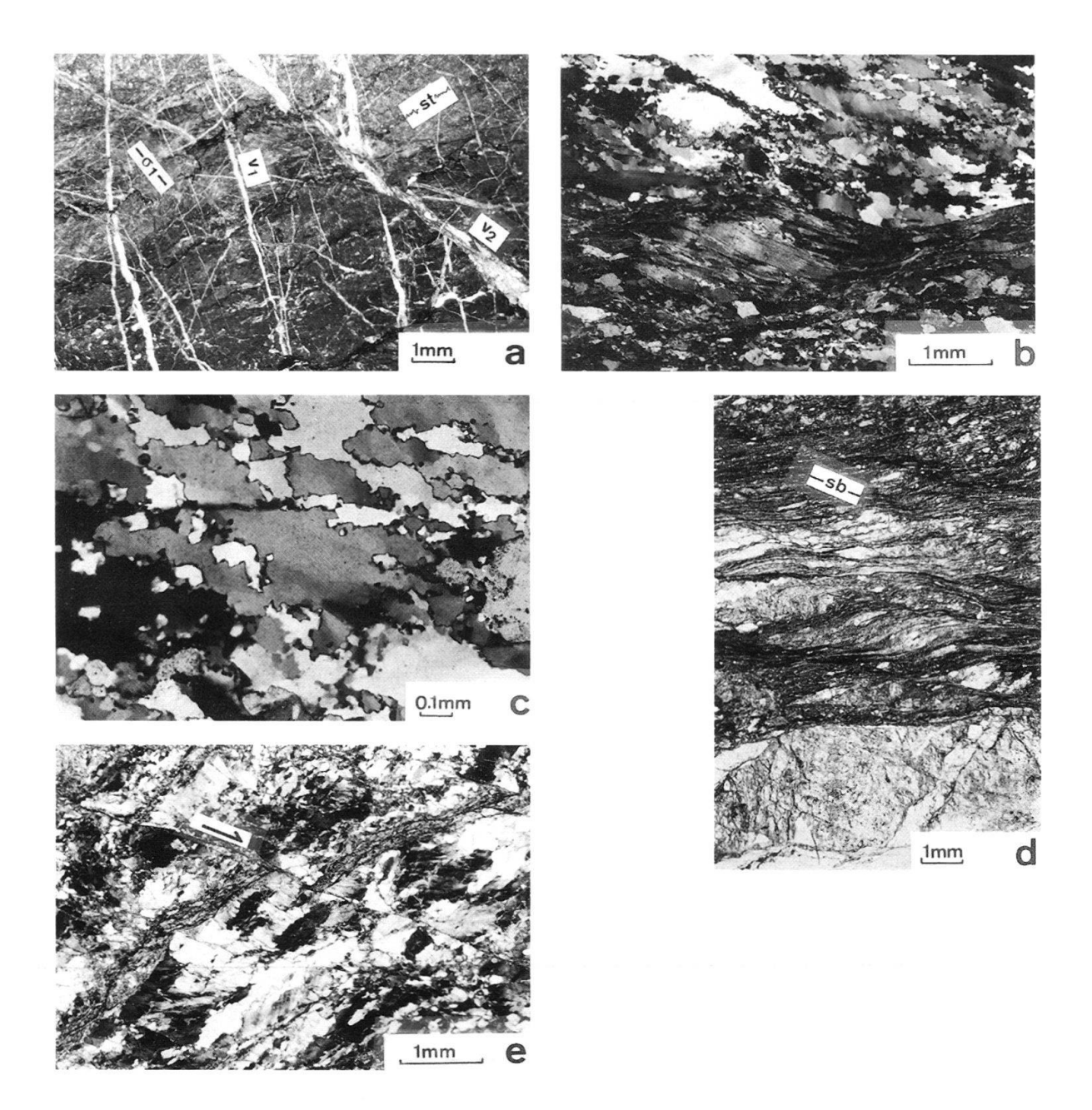


Fig. 6. Thin section micrographs of fault rocks from the Ducan normal fault and the base of the Silvretta nappe. In all micrographs, west is to the left and the fault-zone boundaries are horizontal.

- (a) Cataclastic fault rock of the Ducan normal fault, showing stylolites (st) and two sets of veins, one with undeformed calcite filling ( $v_1$ ), the other including dark zones of cataclastically sheared calcite ( $v_2$ ). The two sets are interpreted as conjugate microfaults. Conjugate microfaults and stylolites indicate orientation of  $\sigma_1$  as shown, compatible with dextral shear sense. Protolith is Middle Triassic limestone. West side of Büelenhorn (coord. 777.9/171.6).
- (b) Mylonite from the base of the Silvretta nappe (first type, see text) formed from a gneissic protolith. Large muscovite "mica fish" (lower left) indicates sinistral (top-west) shearing. Northwest of Piz Belvair (coord. 789.7/165.55).
- (c) Quartz microstructure from same sample as in (b). Grain boundary migration led to preferred grain boundary orientations parallel to the foliation plane (horizontal) and at a high angle to the foliation plane (inclined to the right), indicating sinistral (top-west) shearing.
- (d) Mylonitic to cataclastic fault rock from the base of the Silvretta nappe (second type, see text). Shear bands (sb) indicate dextral (top-east) shearing. Cinuos-chel (coord.798.05/168.85).
- (e) Same sample as in (d). Brittle, synthetic Riedel shear offsetting quartz grains in a dextral (top-east) sense.

roughly perpendicular to the bisecting plane of the acute angle included by the two sets of veins. Where the sheared veins offset other veins, the offset is top-east-directed.

Mutual crosscutting relations between veins of the two sets and stylolites (Fig. 6a) indicate that all these structures originate from the same deformation process. It is therefore assumed that the deformation of the fault rock included fracturing events intermittent with periods of pressure solution creep. During the fracturing events, the two sets of fractures formed as conjugate microfaults in response to stresses associated with fault slip. In the periods of pressure solution creep, calcite was solved along the stylolites and deposited in the fractures which opened up to form veins. The veins of the synthetic set (v<sub>2</sub>) were again cataclastically sheared in a subsequent fracturing event. The angular relation between fault-zone boundaries, stylolitic seams, and veins indicates a top-east-southeast shear sense.

The microstructural study of cataclasites from the northwestern part of the Ducan normal fault thus confirms that the sedimentary rocks of the hanging wall were down-thrown towards east-southeast, that is, parallel to the dip of the fault, onto the gneiss of the footwall. Mylonites from the base of the Silvretta nappe along the presumed east-ward continuation of the Ducan normal fault will be described next.

Between Fuorcla Pischa north of Albula pass and Cinuos-chel in the Upper Engadine valley, the Silvretta nappe is formed by ortho- and paragneiss. The amphibolite-facies metamorphism of these rocks is of Variscan age (370-350 Ma, Maggetti & Flisch 1993). They overlie Jurassic and Cretaceous sediments of the Ela nappe. Thin slivers of Triassic dolomite and cargneule occur in between ("Subsilvrettide Linsen", Fig. 7, Heierli 1955). Mylonites with a clear foliation and stretching lineation, derived from gneissic protoliths, occur along the base of the Silvretta nappe. The mylonites have a thickness of a few metres to several tens of metres. They can be distinguished from the amphibolite-facies pre-Alpine gneisses by their lower-temperature, greenschist-facies overprint. The foliation of the mylonites dips towards north at different angles, mostly between 30° and 50°, parallel to the base of the Silvretta nappe, and the stretching lineation trends east to southeast. Two types of mylonites were observed within the same fault zone, characterized by a distinctly different deformational behaviour of quartz. Figures 6b and c represent the first type of mylonite. Crystal plastic flow in quartz aggregates is accommodated by extensive and pervasive syntectonic recrystallization. Both subgrain rotation and grain boundary migration recrystallization are observed, the latter mechanism leading to preferred grain boundary orientations parallel and at a high angle to the foliation plane (Fig. 6c). Mica fish (Fig. 6b), asymmetric porphyroclasts, shear bands, grain boundary preferred orientation, and crystallographic preferred orientation indicate a top-west to top-northwest sense of shear for these mylonites. A coaxial component of the deformation is indicated by sets of conjugate shear bands with opposite sense of displacement.

The second type of mylonite (Fig. 6d, e) has microstructures indicative of distinctly lower temperatures. In these mylonites, recrystallization of quartz is restricted to narrow bands. Outside of these bands, old quartz grains exhibit undulous extinction and contain deformation lamellae; often they are fractured. Cataclastic shear fractures are common (Fig. 6e). Crystallographic preferred orientation in a narrow recrystallized quartz band, grain shape preferred orientation, asymmetric porphyroclasts, pressure shadows and shear bands (Fig. 6d) indicate a top-east to -southeast movement. The mylonites of this second type obviously formed near the frictional-viscous transition (Schmid & Handy

1991) and overprinted the dynamically recovered and recrystallized mylonites of the first type.

The mylonites which formed at higher temperatures, indicating top-west to top-north-west shear, are interpreted to be related to initial detachment and thrusting of the Silvretta nappe. The younger, lower-temperature, top-east mylonites to cataclasites are interpreted as resulting from back-slipping of the Silvretta nappe towards east, along the original thrust. This surface acted as a prolongation of the Ducan normal fault towards the east and towards greater depth.

### 3.1.5 D<sub>3</sub> folding in the Silvretta nappe

The contours of the Ducan normal fault in Figure 5 outline an east-trending, open synform with an axis south of Bergün. Other, more gentle east- to southeast trending folds affecting the Ducan normal fault are outlined further north. These folds represent a second folding phase in the Silvretta nappe, associated with the third regional deformation event (D<sub>3</sub>). A steeply dipping, west-northwest striking cleavage in sandstones and conglomerates of the Chazfora and Fuorn Formations at the base of the Ducan sedimentary sequence can be ascribed to this folding phase. These clastic sediments are often devoid of a cleavage related to D<sub>1</sub> folding so that the D<sub>3</sub> cleavage is the oldest penetrative structure observed. This cleavage is almost perpendicular to the axes of D<sub>1</sub> folds. D<sub>3</sub> cleavage also overprints Fuorn-Formation-derived cataclasites along the Ducan normal fault at Büelenhorn. This gives additional evidence for a post-normal-faulting (post-D<sub>2</sub>) age of these folds.

In summary, we can distinguish three deformation phases in the southwestern Silvretta nappe, of which the first includes top-west to top-northwest thrusting and related folding around northeast-striking axes, the second, top-east-southeast normal faulting and the third, additional shortening accommodated by east- to southeast-striking folds. We arrive at an explanation for the relationship between Silvretta basal thrust and Ducan syncline that is different from the one of Trümpy (1980): in our view, the Ducan syncline was not formed before the detachment and thrusting of the Silvretta nappe, but during this process. It is true that the Ducan syncline is truncated in the southwest by the basal surface of the Silvretta nappe. This basal surface, however, does not represent the original thrust but rather a segment of the D<sub>2</sub> Ducan normal fault.

#### 3.2 Ela nappe

### 3.2.1 General description

The Ela nappe is a detached and intensely folded sedimentary sequence. It underlies the Silvretta nappe to the south. The Carnian Raibl Group (dolomite, shale, sandstone and evaporite-derived cargneule) forms the décollement horizon at the base of the nappe. Norian Hauptdolomit is the relatively competent "backbone" of the nappe, whereas Rhaetian Kössen Formation and Lower to Middle Jurassic Allgäu Formation are dominated by shales, marls and limestones which generally are strongly folded. Thus the rocks of the Allgäu Formation are particularly well suited for structural analysis. Upper Jurassic and Cretaceous formations, including radiolarian chert, Aptychus limestone and Palombini shale, occur in the topmost parts of the nappe, immediately below the base of the

Silvretta nappe. They are separated from the latter by thin lenses of Triassic rocks, referred to as "Subsilvrettide Linsen" earlier. We subdivide the Ela nappe into an upper unit (Üertsch element) and a lower unit (Compass element, see Fig. 2, small map). The Compass element includes the "Gualdauna-Schuppe" as defined by Heierli (1955) and Eberli (1985) and the overlying Allgäu Formation of Igl Compass (Fig. 2, coord. 782.7/162.6). We chose such a subdivision because a major thrust surface is located between the Allgäu Formation of Igl Compass and the overlying Triassic dolomite of Piz Üertsch. This thrust was in part overprinted by low-angle normal faulting (see below).

In the northwestern part of the map (Fig. 2), the thickness of the Ela nappe decreases until it is represented by only a few metres of limestone in the (recently destroyed) outcrop at Belfort near Tiefencastel (Fig. 2; coord. 765.9/171.1; Trümpy 1980, p. 237). The geometric relations in this area, although badly exposed, suggest that the Ela nappe is continuous with the Rothorn nappe ("Rothornschuppe", Brauchli 1921) exposed in the northwestern corner of the map area (Fig. 2). The latter comprises a gneissic basement and its Triassic cover.

Three generations of folds can be distinguished in the Allgäu Formation of the Ela nappe between Bergün and the Albula pass. All three are observed on different scales, from thin-section to cross-sectional view of the nappe (Fig. 3b).

## 3.2.2 D<sub>1</sub> folding and thrusting in the Ela nappe

Early folds in the Allgäu Formation of the Ela nappe are tight to isoclinal and associated with a well-developed axial plane cleavage and a mostly east-west trending lineation. This lineation is a cleavage-bedding intersection lineation but at the same time a stretching lineation as indicated by deformed markers, such as conglomerate pebbles and belemnite rostra. In contrast to the Silvretta nappe, lineation and cleavage are ubiquitous throughout the Ela nappe. Fold hinges are rarely found but always oriented parallel to the lineation. In general, they strike about eat-west and gently plunge towards east or west (Fig. 7a). The facing of  $D_1$  folds is generally towards south in those parts of the Ela nappe where the stratigraphic succession is in an overall upright position. Curving  $D_1$  fold hinges or sheath folds have not been observed in the Ela nappe, in contrast to the underlying Err-Carungas nappe where they are common (see below).

The strong overprinting of D<sub>1</sub> folds by younger structures, most importantly recumbent D<sub>2</sub> folds, makes it difficult to reconstruct the large-scale geometry of D<sub>1</sub>. Nevertheless a reconstruction is attempted in Figure 8. Even after retro-deformation of D<sub>2</sub> folds, a two-stage evolution of D<sub>1</sub> structures needs to be proposed in order to explain the geometric relations. We assume that the south-facing folds (see above) were formed in an early stage of D1 (Fig. 8a). In the Ela nappe, such south-facing D<sub>1</sub> folds are restricted to outcrop-scale structures and are only found in the Allgäu Formation. However, large south-facing D<sub>1</sub> folds with basement in the anticlinal cores and sediments in synclines are found in the southern part of the Rothorn nappe (NW corner of map, Fig. 2, coord. 764/176), the presumable northwestern continuation of the Ela nappe. These were already described by Brauchli (1921). The Üertsch element of the Ela nappe can be viewed as a south-facing, isoclinal syncline with a thick normal limb and an extremely thinned inverse limb, represented by the "Subsilvrettide Linsen". (According to Heierli 1955 and Pittet 1993, these slivers include inverse-lying stratigraphic sequences.) The internal

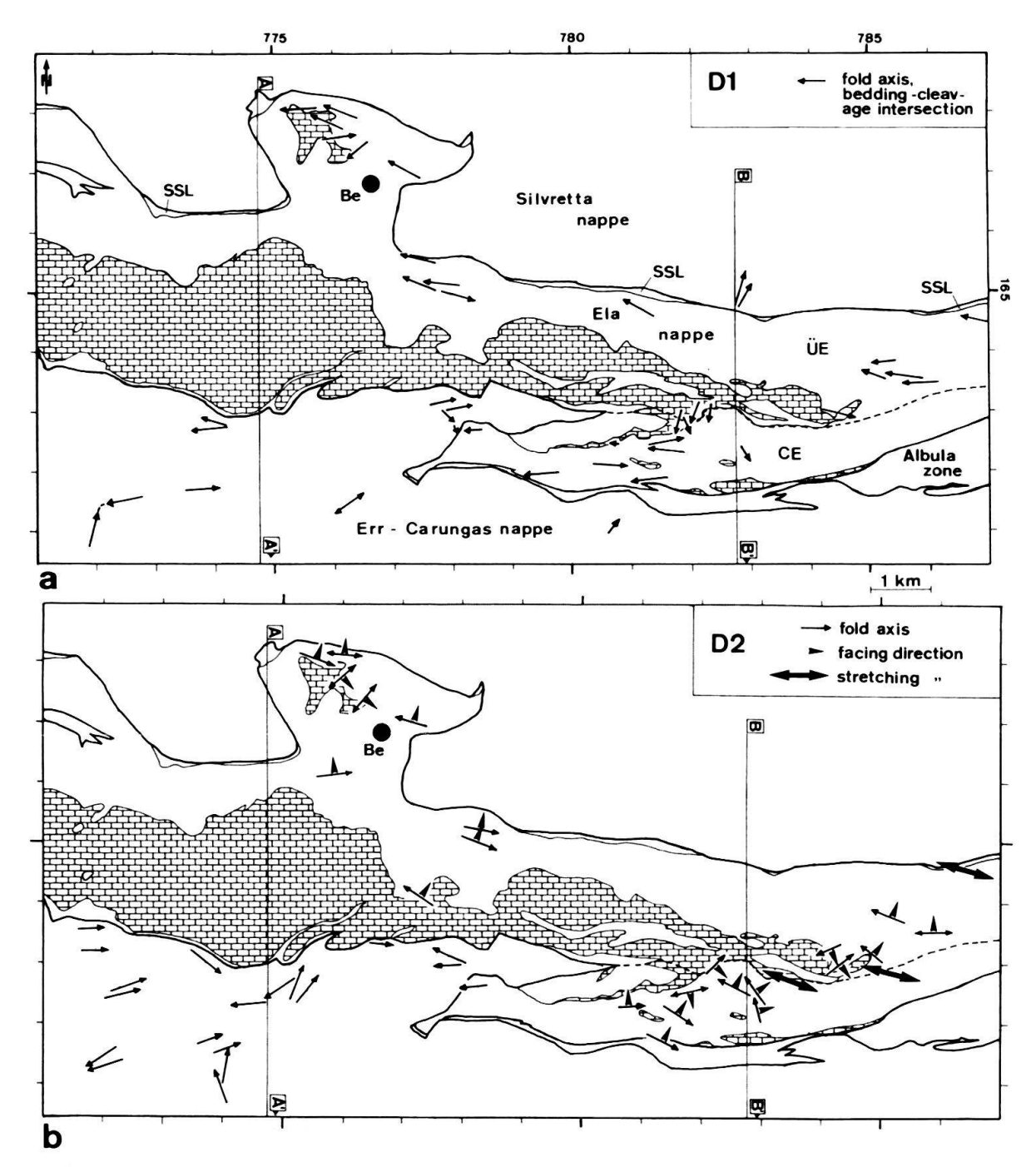
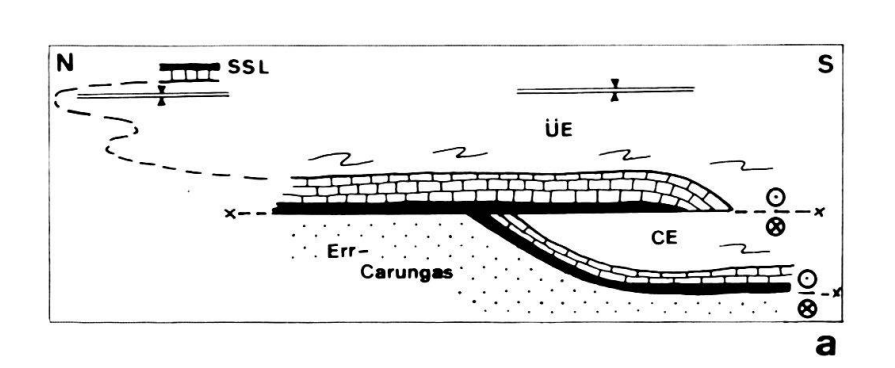


Fig. 7. Orientations of  $D_1$  and  $D_2$  fold axes in the Ela and northern Err-Carungas nappes. Arrows indicate plunge direction of fold axes, length of arrow correlates to plunge angle (longest arrows for horizontal fold axes, shortest arrows for subvertical fold axes). Be, Bergün; CE, Compass element; SSL, "Subsilvrettide Linsen"; ÜE, Üertsch element; brick signature for Hauptdolomit of the Ela nappe; traces of cross sections of Fig. 3 are indicated; other localities can be identified by comparison with Fig. 2.

- (a)  $D_1$  folds. Note that these trend northeast in the Silvretta nappe and in the Err-Carungas nappe, and that the Ela nappe represents a "channel" of east-west-trending  $D_1$  folds between the two other nappes. Only in the basal part of the Allgäu Formation of the Ela nappe, near the underlying Hauptdolomit, more north-south trending  $D_1$  folds occur.
- (b)  $D_2$  folds. Arrows without shaft indicate facing directions of  $F_2$  folds. Facing is either towards north or south for east-west-trending folds, and generally towards northeast to southeast for more north-south-trending folds. Thick arrows with two heads indicate stretching directions in metre-scale extensional shear zones in the Allgäu Formation.



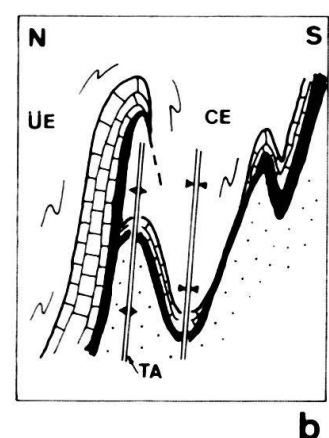


Fig. 8. Diagrammatic cross sections showing evolution of  $D_1$  structures in the Ela nappe along profile of Fig. 3b. Legend of lithologies and fold axial surfaces as in Fig. 2.

- (a) Early stage of  $D_1$ : the Ela nappe is thrust over the Err-Carungas nappe from east to west, perpendicular to the plane of the section. An internal thrust forms in the Ela nappe, bringing the Üertsch element (ÜE) over the Compass element (CE).  $D_1$  folds forming during this stage face towards south. The "Subsilvrettide Linsen" (SSL) are interpreted as representing the extremely thinned inverse limb of a south-facing syncline comprising the entire Üertsch element.
- (b) Late stage of  $D_1$ : structures in the Ela nappe are steepened by upright folds, the Tschitta anticline (TA) and a syncline south of it. The area was later overprinted by recumbent  $D_2$  folds, leading to the geometry seen in Fig. 3b.

thrust within the Ela nappe that brought the Üertsch element over the Compass element is also ascribed to this stage (Fig. 8a). We relate the south-facing  $D_1$  folds and the internal thrust to formation and transport of the Ela nappe, and assume that the direction of shearing was towards west. This is indicated by the general east-west orientation of the  $D_1$  stretching lineation not only in the Ela nappe but also in the over- and underlying units. Note that the termination of the Compass element towards north (Fig. 8a) has to be interpreted in terms of a lateral ramp in this case.

How can the southward facing direction of  $D_1$  folds be reconciled with westward thrusting? We assume that the parallelism of the fold axes and stretching lineations is the result of a systematic rotation of the former towards the shearing direction. If folds had been initiated with axes perpendicular or oblique to the shearing direction, and with a facing towards west, the present southward facing requires that the fold axes were rotated uniformly and counterclockwise in map view.

The folds described above have axial planes subparallel to the thrust surface along which the Ela nappe was emplaced on the Err-Carungas nappe, and also to the internal thrust of the Üertsch element over the Compass element. A different class of  $D_1$  folds must have developed after the Ela nappe had been emplaced on the Err-Carungas nappe. These younger folds deform the basal thrust of the Ela nappe (Fig. 3b, Fig. 8b). The folds are also attributed to  $D_1$ , because a distinction between the two sub-generations is only possible in a few places, and because they probably formed in a continuous process. One of the younger  $D_1$  folds is the east-plunging Tschitta anticline. It forms a half-window in which Upper Jurassic to Cretaceous sediments of the Err-Carungas nappe appear under the Ela nappe (Fig. 2, coord. 779/163, and Fig. 3b). The younger folds are

responsible for the general steepening of rock units not only in the Ela nappe, but also in the northernmost parts of the Err-Carungas nappe. In the following, this belt of steep units will be termed "Albula steep zone".

The development of  $D_1$  structures in the Ela nappe can be summarized as follows: the Ela nappe was detached from its basement along the Carnian evaporite, and transported towards west. Early  $D_1$  folds and an internal thrust of the Üertsch element over the Compass element evolved during this detachment and transport of the nappe. Later on, after emplacement of the Ela nappe on the Err-Carungas nappe, upright folds developed, leading to a general steepening of rock units (Albula steep zone).

### 3.2.3 D<sub>2</sub> "collapse folding" and minor normal faulting in the Ela nappe

 $D_2$  folds of the Ela nappe are typically open to tight, rarely isoclinal with subhorizontal to moderately dipping axial surfaces (Figs. 9a, 10b). In pelitic lithologies, they are associated with a solution- or crenulation cleavage. Open  $D_2$  folds often have no axial-plane cleavage. Many of the  $D_2$  fold axes are oriented east-west, parallel to  $D_1$  folds and the  $D_1$  stretching lineation (Figs. 7b, 10a). However, the trend of  $D_2$  folds is highly variable, and almost north-south striking axes occur as well. Figure 9a shows  $D_2$  folds trending obliquely to  $D_1$  structures and therefore deforming the  $D_1$  lineation. The facing directions of east-west trending  $D_2$  folds vary depending on their position in respect to upright  $D_1$  folds like the Tschitta anticline.  $D_2$  folds face north on the northern limbs of upright  $D_1$  anticlines, and south on the southern limbs (Fig. 3b). The facing direction of more north-south oriented  $D_2$  folds is generally towards east (Fig. 7b).

The most spectacular and obvious D<sub>2</sub> structure is the east-west-striking, north-facing, recumbent Ela fold marked by the thick Hauptdolomit of Piz Ela. Previously this fold was interpreted to be related to the formation of the Ela nappe as a recumbent fold nappe ("Stirnfalte" or frontal fold of the older authors, e. g. Heim 1922, Fig. 227; Eugster 1923, Fig. 32). However, the fold clearly overprints D<sub>1</sub> folds, and the D<sub>1</sub> cleavage is folded around its hinge. It must therefore be younger than D<sub>1</sub>, as was already proposed by Spitz & Dyhrenfurth in their very remarkable article on the tectonics of the Ela – Silvretta area (1913, p. 498).

Large-scale  $D_2$  folds deform the base of the Silvretta nappe west of Bergün, representing the preserved original thrust of the Silvretta over the Ela nappe formed during top-west to top-northwest displacement. For example Figure 3a shows the Silvretta basal thrust folded around the Ela  $D_2$  fold (see also cross section of Piz Ela in Trümpy 1980, p. 238). However, further east where the Silvretta base was reactivated by top-east displacement and where it coincides with the continuation of the Ducan normal fault, axial surfaces and cleavage of  $D_2$  folds become subparallel to the Silvretta base. Folding of the Silvretta base by  $D_2$  is no more observed. This is one piece of evidence amongst others indicating that  $D_2$  folding in the Ela nappe postdates the emplacement of the Silvretta on the Ela nappe, but is contemporaneous with the extensional faulting in the Silvretta nappe.

A crucial outcrop for understanding the relation between  $D_2$  folds and extensional faults at a smaller scale is Igl Compass north of Albula pass (Fig. 11). Here, the  $D_2$  fold axes strike north-northwest. The Jurassic strata of Igl Compass form a large, northeast-facing  $D_2$  anticline with a moderately northeast-dipping axial surface. Along the fault

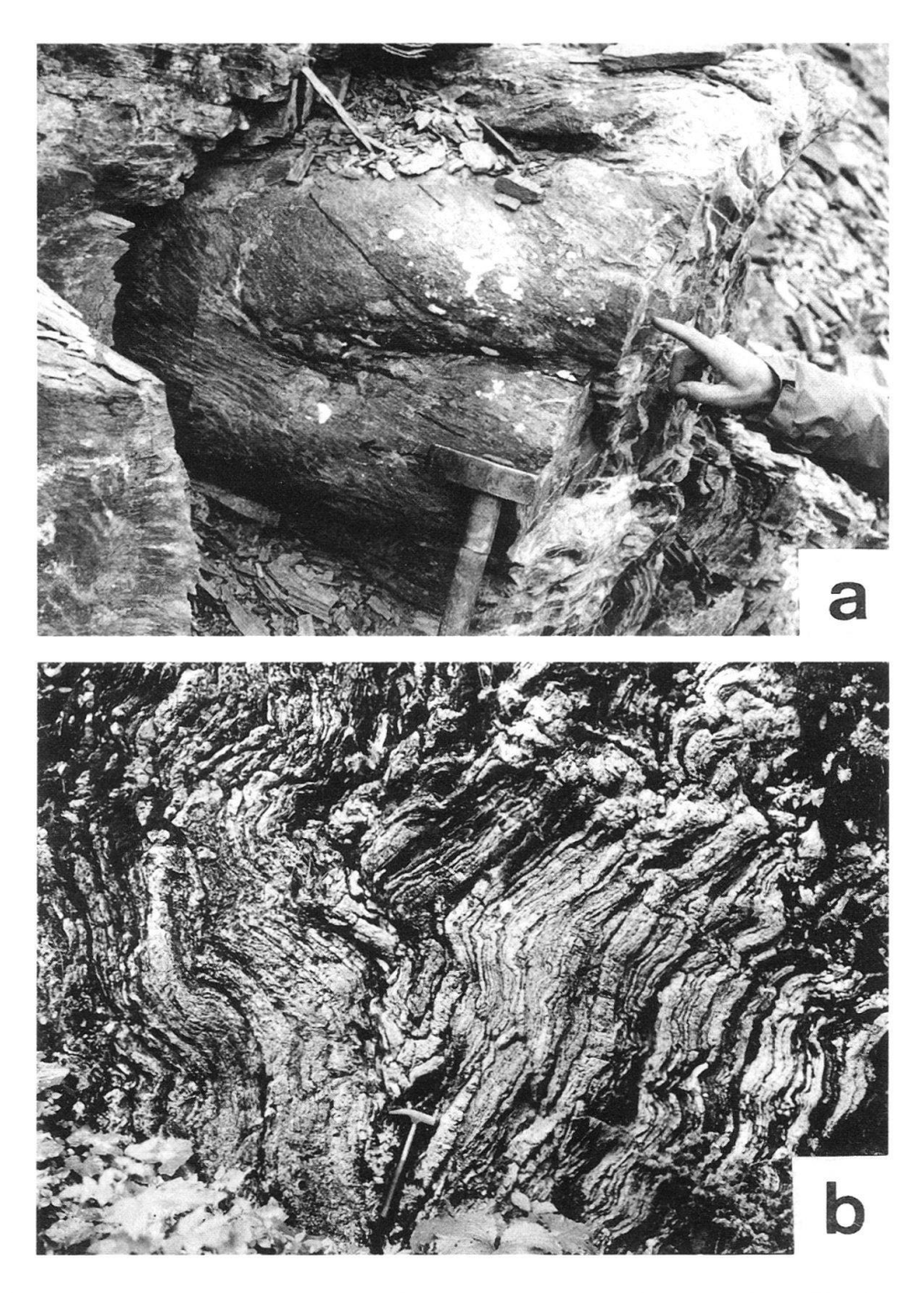


Fig. 9. (a)  $D_1$ – $D_2$  overprinting in the Ela nappe. Recumbent  $D_2$  folds in limestone of the Allgäu Formation on the south side of Igl Compass (coord. 782.9/162.5). The marked lineation curving around the fold hinges is the  $D_1$  stretching- and cleavage/bedding intersection lineation.

(b)  $D_1$ – $D_2$  overprinting in the Err-Carungas nappe. Upright  $D_1$  synform in Upper Jurassic radiolarite of the Carungas zone, overprinted by weak  $D_2$  folds with subhorizontal axial surfaces. The  $D_1$  fold is a minor fold in the northern limb of the Tschitta anticline (compare Fig. 3b). Outcrop under the third railroad bridge over the road from Bergün to Albula pass near Punt Ota (coord. 777.6/163.3).

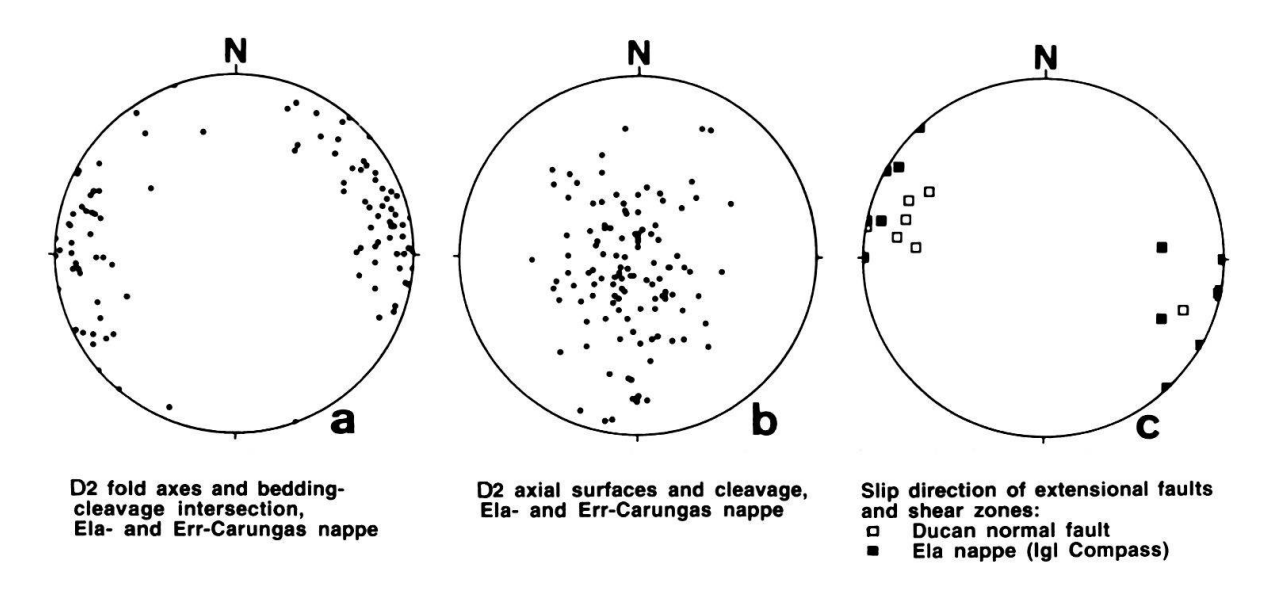


Fig. 10. Equal-area, lower-hemisphere stereographic representation of D<sub>2</sub> structures in Ela nappe and Err-Carungas nappe. Note parallelism in (c) between slip direction of Ducan normal fault (open symbols) and D<sub>2</sub>-related shear zones and normal faults in the Ela nappe (filled symbols). For further explanation see text. After Froitzheim (1992).

contact shown in the upper right corner of Figure 11, the Jurassic strata are overlain by Triassic dolomite. This contact is a top-to-the-east-southeast directed normal fault, as indicated by asymmetric shear-band/foliation relations and drag folds in mylonitic limestone along the fault. The normal fault overprints a former thrust, the thrust of the Üertsch element over the Compass element (see above). As a result, it has older rocks in the hanging wall than in the footwall. It is subparallel to the Ducan normal fault further north and has the same slip direction (Fig. 10c). Therefore it is interpreted as a normal fault of the same generation as the Ducan fault. Tentatively, a second fault in a deeper structural level is also interpreted as a normal fault (Fig. 11). Parasitic D<sub>2</sub> folds subordinate to the northeast-facing anticline are seen between the two faults. These minor folds are associated with extensional shear zones generally located in the overturned limbs of the folds and resulting in stretching and thinning, or complete disruption, of the overturned limbs. The regular arrangement of the shear zones in the overturned limbs of the folds makes it likely that both kinds of structures developed together.

The development of the Igl Compass structure is explained in Figure 11b. Because Igl Compass is located near the hinge of a large-scale, upright D<sub>1</sub> fold with an east-dipping axis (the Tschitta anticline), it is assumed that the strata dipped east or northeast before D<sub>2</sub>. Deformation in a broad shear zone with a normal-fault geometry, dipping toward east at a shallower angle than the bedding, resulted first in shortening and buckling of the competent layers. Later, with progressive deformation, the layers rotated into the extension field of the incremental strain ellipse and were disrupted by extensional shear zones. In summary, the geometric relations between shear zones and folds at Igl Compass suggest that fold formation resulted from top-to-the-east-southeast directed extensional shearing, affecting initially east- to northeast-dipping layers (Froitzheim 1992).

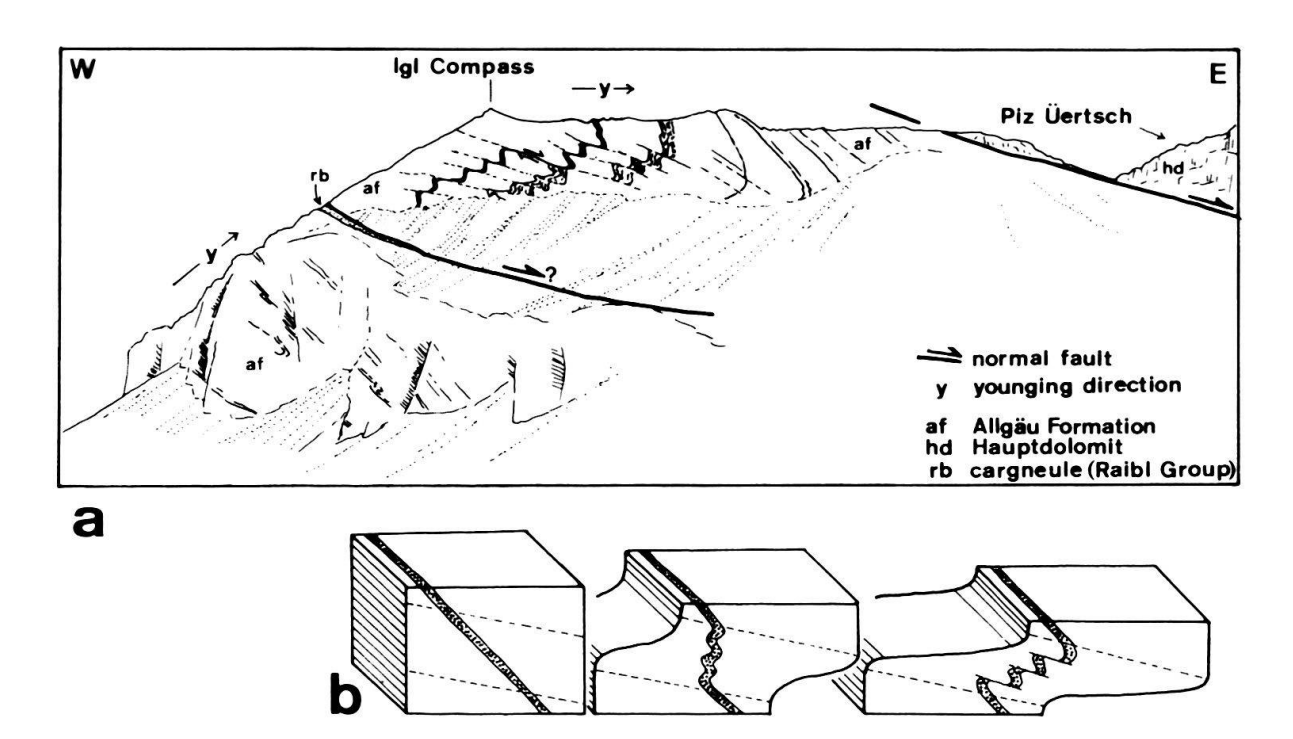


Fig. 11. D<sub>2</sub> structures at Igl Compass (Ela nappe north of Albula pass). (a) View of Igl Compass from south. Note regular arrangement of extensional shear zones in hinges of folds, suggesting that folds and shear zones originated from continuous process. (b) Model for continuous development of D<sub>2</sub> folds and extensional shear zones by top-east directed shearing deformation. Stippled layer is first shortened, then extended. After Froitzheim (1992).

This explanation can be extended to the  $D_2$  folds of the Ela nappe in general (Froitzheim 1992): These folds reflect east-southeast directed extension whereby previously steepened layers (Albula steep zone formed during  $D_1$ ) were shortened in a subvertical direction.

## 3.2.4 D<sub>3</sub> folding in the Ela nappe

D<sub>3</sub> folds are open folds with steeply dipping axial surfaces, affecting the Silvretta, Ela and Err-Carungas nappes together. D<sub>3</sub> fold axes and axial surfaces in the Ela nappe strike east to southeast. A cleavage related to D<sub>3</sub> was not observed. The style of D<sub>3</sub> folding is strongly dependent on the lithology of the rocks affected. The thick Hauptdolomit of the Ela nappe west of Bergün is unaffected by D<sub>3</sub> folding while the Allgäu Formation of Piz Blaisun (Fig. 2, coord. 785.7/164.2) is particularly intensely folded by D<sub>3</sub> (Pittet 1993, Unmüssig 1993). The syncline at the summit of Piz Blaisun, with Upper Jurassic radiolarite in the core, is such a D<sub>3</sub> structure. This syncline has a vertical axial surface; others have steeply north- or south-dipping axial surfaces.

The structural analysis of the Ela nappe thus reveals the superposition of three major deformation events. The first is related to westward thrusting and subsequent steepening of the rock units in the "Albula steep zone", the second one to east-southeast directed extension, and the third one to renewed shortening in a north-south to northeast-southwest direction.

## 3.3 Err-Carungas nappe

# 3.3.1 General description

The Err-Carungas nappe includes the "Errdecke s. s.", the "Albulalappen" and the underlying "Carungasdecke" as defined by Stöcklin (1949, Tf. 1, "Tektonische Übersicht"). We treat these units as parts of one nappe, because in Val d'Err (Fig. 2), Carungas zone and Err nappe s. s. are connected by a continuous syncline of Jurassic-Cretaceous sedimentary rocks (Lozza 1990). Important displacement horizons may exist, however, in the lower part of the Carungas zone (G. Eberli, pers. comm.; see also Ring et al. 1990). The basement of the Err nappe s. s. and the "Albulalappen" are formed by Lateto Post-Hercynian granitoids and their wall rocks of gneiss and mica schist. A thin cover of Triassic rocks is preserved on top of this basement and along its northern border near the Albula pass. The Carungas zone is exposed in an eastward-narrowing stripe between the Err nappe s. s. and the "Albulalappen" to the south and the Ela nappe to the north (most of the area labelled "Mesozoic sedimentary rocks" in Fig. 2). This zone is made up of intensely folded, exceptionally thick Upper Jurassic to Cretaceous sedimentary rocks with thin anticlinal cores of Lower to Middle Jurassic, Triassic and basement rocks. In the Middle Jurassic, the area of the present Err-Carungas nappe was the site of dramatic rifting activity. This is documented by erosional hiatuses (Stöcklin 1949), sedimentary breccias with basement clasts, and preserved normal faults. Remnants of a low-angle detachment fault of presumably Middle Jurassic age are found on top of the Err nappe s. s. around Piz d'Err and Piz Jenatsch (Froitzheim & Eberli 1990).

#### 3.3.2 Structural analysis

Because of the complicated rift configuration, the early Alpine (pre-D<sub>2</sub>) deformation of the Err-Carungas nappe is only poorly understood. In pelites and pelitic limestones (e. g. Aptychus limestone) of the Carungas zone, a well developed early cleavage has often completely transposed sedimentary bedding. D<sub>1</sub> folds associated with this cleavage are isoclinal and some of them have the geometry of sheath folds. The orientation of D<sub>1</sub> folds is highly variable, due to their sheath-fold geometry and the strong D<sub>2</sub> overprint. The most prominent D<sub>1</sub> structure of the Carungas zone is the Tschitta anticline. In the east (Fig. 3b) the Tschitta anticline deforms the thrust at the base of the Ela nappe and has an upright, eastwest striking axial surface. Further towards the southwest, the axial surface becomes subhorizontal (Fig. 3a). The continuation of the Tschitta anticline in Figure 3a is hypothetical. In contrast to the sedimentary rocks of the Carungas zone, the pre-Permian basement mass of the Err nappe s. s. is devoid of penetrative D<sub>1</sub> structures (G. Manatschal, pers. comm.).

D<sub>2</sub> structures of the Err-Carungas nappe are similar to those of the Ela nappe: recumbent folds with an axial plane solution cleavage or crenulation cleavage. Typically, recumbent D<sub>2</sub> folds overprint upright D<sub>1</sub> folds in a tpye 3 pattern (Ramsay 1967; Fig. 9b). The frontal fold of Piz d'Err (Fig. 3a, right-hand end of section) is such a major, north-facing D<sub>2</sub> anticline. D<sub>2</sub> folding also affected the boundary between Err-Carungas nappe and Platta nappe: a half-window exposing the Platta nappe in Val d'Err (Fig. 2, coord. 773/160) represents the eroded core of a D<sub>2</sub> fold (Fig. 3a). These folds are interpreted as reflecting vertical shortening of previously steepened layers during east- to southeast-directed extension, just like the D<sub>2</sub> folds of the Ela nappe.

D<sub>2</sub> normal faults similar to those observed in the Silvretta nappe and also, but to a much lesser extent, in the Ela nappe, have recently been found in the Err-Carungas nappe (Weh 1992, G. Manatschal, pers. comm.). Weh (1992) reported a subhorizontal, top-southeast directed cataclastic shear zone near Murtel Trigd (Fig. 2, coord. 779/161) in the northern part of the Err basement and ascribed it to extensional faulting coeval with D<sub>2</sub> folding. It is possible that more such extensional faults and shear zones, related to D<sub>2</sub> deformation, exist in the northern Err-Carungas nappe.

 $D_2$  and  $D_1$  structures are overprinted by upright, open folds with east- to southeast striking and steeply north- to northeast-dipping axial planes ( $D_3$ ).  $D_3$  folds in the Err-Carungas nappe are associated with a weak axial plane solution cleavage. The broad antiformal arch described by the  $D_2$  axial surfaces in Figure 3a is a  $D_3$  structure.

The Err-Carungas nappe thus shows a structural evolution very similar to that of the Ela nappe: early thrusting and folding  $(D_1)$  were followed by recumbent "collapse folding"  $(D_2)$  and by still later, open  $D_3$  folding.

## 4 Sequence of stages of the orogenic evolution

In the preceding paragraphs, we have described the sequence of deformation phases observed in each of the three nappes, Silvretta, Ela and Err-Carungas. We will now combine these data and propose a reconstruction of the regional tectonic evolution, assuming that the deformation phases are related to distinct stages of the orogenic evolution.

#### 4.1 Trupchun phase $(D_1)$ : Cretaceous top-west thrusting and folding

The Trupchun phase includes the  $D_1$  thrusts and folds of the three nappes. It is named after Val Trupchun, situated at the western end of the Ortler nappe (see chapter 5.3), where structures of this phase are particularly well preserved.

We assume that the  $D_1$  folds of the Silvretta nappe, such as the Ducan syncline, were formed during initial detachment and westward transport of the nappe. Their orientation – northeastern strike and northwestward facing – fits well together with the westward to northwestward direction of thrusting, as indicated by the lineation in the older, higher-temperature mylonites at the base of the Silvretta nappe.  $D_1$  folds in the Ela nappe are more complicated. In the Ela nappe,  $D_1$  includes two kinds of folds: first, east-striking, south-facing folds with axial planes subparallel to the basal thrust of the Ela nappe, and second, also east-striking, but upright folds deforming the basal thrust (Fig. 8).

The first "sub-generation" is comparable and probably coeval with the  $D_1$  folds of the Silvretta nappe. The different strike of the fold axes, northeast in the relatively rigid Silvretta nappe and east in the ductile Ela nappe, can be explained with a rotation of fold axes of the Ela nappe into the shear direction. The beginning of such a rotation is noticed in the southwestern part of the Ducan syncline, where fold axes curve around from northeast-striking to north- and northwest-striking. A possible explanation for the anti-clockwise rotation of fold axes is a different rate of top-west shearing, higher in the north and lower in the south. This implies that northern parts of the nappe pile advanced towards west relative to more southern parts.

The slightly younger, upright  $D_1$  folds in the Ela nappe have no counterpart in the Silvretta nappe. These upright folds led to a steepening of all rock units in the Albula